Available online at www.sciencedirect.com

ScienceDirect

Mendeleev Commun., 2022, **32**, 825–827

Mendeleev Communications

Synthesis and characteristics of copper(II) trimesate composites with thermal decomposition products of the coffee and tea waste

Oxana V. Kharissova,*[a] Vladimir A. Zhinzhilo,[b] Iman S. Gubaeva,[b] Igor E. Uflyand[b] and Boris I. Kharisov[a]

[a] *Universidad Autónoma de Nuevo León, 66455 San Nicolás de los Garza, Nuevo León, México.*
E-mail: bkhariss@hotmail.com
[b] *Department of Chemistry, Southern Federal University, 344090 Rostov-on-Don, Russian Federation*

DOI: 10.1016/j.mencom.2022.11.039

Composites containing a metal–organic framework of copper(II) 1,3,5-benzenetricarboxylate with activated carbons from pyrolysis of the coffee bean as well as green and black tea waste have been found suitable for recovery of the organic dyes Congo red and methylene blue from their aqueous solutions with a maximum adsorption of 180 mg g^{-1}.

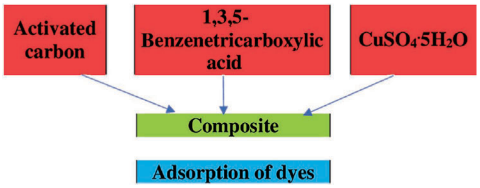

Keywords: composite, metal–organic framework, activated carbon, extraction, adsorbent, pollutant.

Discharge of dyes from the textile, leather, paper and chemical industries into the environment represents a serious problem, so the extraction of toxic colorants as manmade pollutants from the environmental media is of particular importance. Their adsorption on activated carbon has been widely used due to the adsorbent efficiency, ability to separate a wide range of chemical species, simple design and economic attractiveness.[1] However, commercially available activated carbon is produced from high cost non-renewable raw materials like coal or the inexpensive but technologically inconvenient ones such as wood. Therefore, researchers look for cheaper, more efficient and environmentally friendly sorbents from accessible materials.

Another task is the disposal of human consumption waste and crop residues that can be cheap renewable precursors for activated carbon,[2] examples are pomelo,[3] orange[4] and banana[5] peel, tomato waste,[6] *Macadamia* nut shells,[7] corncob,[8] *Ziziphus lotus* stone[9] as well as rice husk.[10] Particular attention is paid to the recycling of coffee and loose-leaf tea waste.[11–13] Since 18–20 billion cups of tea are drunk daily in the world, tea producers face the challenge of disposing of the used tea leaves after their extraction as a part of the global problem of food loss and waste, which is estimated to reach 2.1 billion tons of wasted food by 2030 and incurs losses of *ca*. \$1.5 trillion worldwide.[14] However, investigations of the application of the used coffee grounds and loose-leaf tea waste as precursors for activated charcoal are lacking.

Properties of materials based on metal–organic frameworks (MOFs)[15–17] are typically optimized using their nanocomposites with carbon materials.[18–20] These composites has a narrow pore size distribution and their doping with heteroatoms like Fe, Co or Cu improves the sorption properties, which allows these compounds to successfully compete with carbon derivatives. Thus, porous structures from various types of MOFs and their compositions with carbon can be applied to solve dedicated practical problems.

The aim of this work was to test the coffee[†] and tea consumption waste[‡] as precursors to activated carbon[§] with its following application in the MOF composite materials.

The composites were synthesized from the carbon samples, trisodium 1,3,5-benzenetricarboxylate (sodium trimesate) and $CuSO_4 \cdot 5H_2O$ by the *in situ* method in two steps.[¶] The activated carbon samples and resulting composites were characterized by IR spectroscopy, porosity measurements and scanning electron microscopy (SEM).[††] Adsorption of dyes on the composites was investigated according to the known technique.[21]

In the IR spectra of the activated carbon samples obtained from the waste of green tea, black tea and coffee the same characteristic bands are present, which indicate their identical chemical nature. A wide band at 3480–3400 cm^{-1} corresponds to

---

[†] Coffee grounds were washed several times with hot distilled water (60 °C) under suction on a Buchner funnel using a paper filter with a density of 80 g m^{-2} and a pore size of 8–12 μm until the filtrate pH reached 6.1. Then the product was dried in an oven at 105 °C for 24 h, crushed, sieved to obtain 250–800 μm particles and stored in clean dry flasks.

[‡] Clean ripened tea leaves were boiled in distilled water several times until the supernatant remained colorless. Then the washed material was dried in an oven at 60 °C, crushed, sieved, impregnated with 85% phosphoric acid and kept at 100 °C for 3 h.

[§] The carbon precursors were placed in a tube furnace, evacuated to a residual pressure of 10 Torr, heated from room temperature to 650 °C at a heating rate of 5 °C min^{-1} and kept at this temperature for 1 h. The product was washed with 0.1 M HCl and then distilled water, dried in an oven at 110 °C for at least 12 h, crushed and stored in a desiccator for further use. Before the use, the coal was dispersed using sieves with a mesh size of 0.07–0.6 mm. Particles with a size of 0.2–0.6 mm were discarded, while the ones with a size of 0.08–0.15 mm (89.5 wt% of the initial product) were used in further tests.

[¶] Sodium trimesate was obtained according to the known procedure.[21] The calculated amount [10 wt% of the planned weight of copper(II) trimesate] of carbon obtained by the pyrolysis of the coffee or tea waste was mixed with distilled water (1 : 50 wt/wt), agitated on a magnetic stirrer for 3 h and added to the solution of sodium trimesate with continuous stirring for 30 min. A solution of $CuSO_4 \cdot 5H_2O$ (30 mmol) in water (20 ml) was added to the mixture continuously dropwise with intensive agitation. As a result, a gray-blue gel was formed and further subjected to sonication at ambient temperature for 12 h. The final product was separated by centrifugation at 8000 rpm, washed with water, dried in air and then in an oven at 110 °C.

[††] IR spectra were recorded on a Varian Excalibur 3100 FTIR spectrometer using KBr pellets and the Soft Spectra data analysis program. SEM was performed on a Zeiss Crossbeam 340 platform.

bending vibrations of hydroxyl groups linked by hydrogen bonds, a weak band at ~1730 cm^{-1} refers to bending vibrations of the carbonyl group of ketones, aldehydes or lactones, while an intense band at 1590 cm^{-1} corresponds to vibrations of C=C bonds in the aromatic nucleus. The bands at *ca*. 1645, 1460 and 1385 cm^{-1} characteristic of the vibrations of carboxyl groups are also clearly visible. Due to the presence of acidic groups in the samples in a neutral medium, carbon could lower the initial pH of the aqueous solution from 6.8 to 4.6, therefore it was necessary to bring the pH to its initial value for further dye adsorption measurements.

The activated carbon obtained from coffee beans showed the largest internal surface area, surpassing that of the standard one made industrially from birch wood (Table 1).

Each carbon sample has a developed inner surface due to numerous internal partitions and channels (Figure 1). Note, that the green tea leaf carbon has dense texture with channel size < 5 μm, while the coffee bean carbon has thin partitions and much more developed channel system with small dimensions of the 10 × 10 μm order. The black tea leaf carbon is less compact in texture than the green tea one, but has fewer pores about the same diameter as the coffee bean carbon.

In the composites obtained further from the carbons from the waste of green tea, black tea and coffee, designated as composites **1**, **2** and **3**, respectively, microcrystals of the formed MOF structure are located on the surface of the pores and channels of activated carbon, but do not close them, this creates favorable conditions for adsorption. Note, that the size of MOF crystals in the composites is always smaller than the one of the MOF structures in the absence of activated carbon.

In general, IR spectra of the composites retains the pattern of copper(II) trimesate.[21] However, the doublet at ~750 cm^{-1} is shifted in the composites by 30 cm^{-1} towards an increase in the wavenumber, while its intensity is 12% higher. The characteristic bands of copper(II) trimesinate at 1350–1620 cm^{-1} are shifted for the composites by 10–20 cm^{-1}, while their intensity is similar.

The maximum adsorption capacity was determined by a series of experiments varying the dose of the composite with constant stirring for 3 h, the maximum value of adsorption was found to be 180 mg g^{-1}. The adsorption capacity of the composites with respect to different organic dyes decreases as the following: composite **3** > composite **2** > composite **1**. To investigate the kinetics of the adsorption, a graph lg($q_e - q_\tau$) *vs*. time was constructed, which represented a straight line corresponding to a preudo-first order model (Table 2). The linear correlation coefficients R^2 for the alternative pseudo-second order and intraparticle diffusion models allow us to state that the adsorption processes are in poor agreement with them.

Table 1 Physical characteristics of the activated carbons obtained.

Origin of activated carbon	Bulk density/ g dm^{-3}	Internal surface area/m^2 g^{-1}	Total pore volume/cm^3 g^{-1}
Green tea leaves	326	202	0.31
Black tea leaves	317	217	0.34
Coffee beans	298	269	0.78
Birch wood (standard)	458	196	0.28

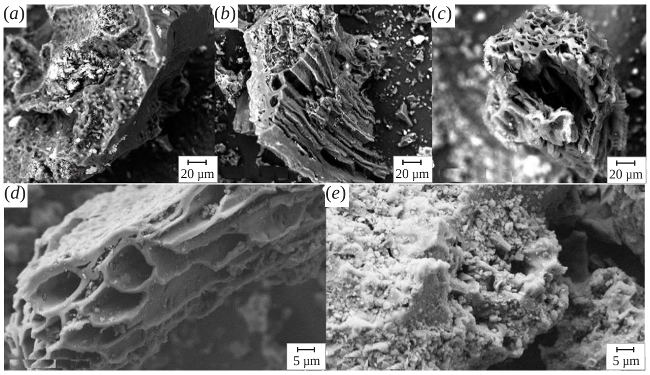

Figure 1 SEM images of activated carbon samples obtained from (*a*) green and (*b*) black tea leaves, (*c*,*d*) from coffee beans as well as (*e*) of a composite based on the carbon from coffee beans.

Table 2 Kinetic parameters for different adsorption models: pseudo-first and pseudo-second order as well as the intraparticle diffusion one.

Pseudo-first order model

Composite	Dye	Rate constant k_1/ min^{-1}	Equilibrium concentration q_e/mg g^{-1}	R^2
1	Congo red	0.65	35.84	0.956
2		0.93	38.04	0.984
3		1.03	39.12	0.993
1	Methylene blue	0.49	35.68	0.959
2		1.06	37.74	0.923
3		1.2	38.6	0.899

Pseudo-second order model

Composite	Dye	Rate constant k_2/ g mg^{-1} min^{-1}	Initial adsorption rate h/ mg g^{-1} min^{-1}	R^2
1	Congo red	0.21	2.76	0.809
2		0.08	0.115	0.788
3		0.19	2.9	0.924
1	Methylene blue	0.12	0.152	0.631
2		0.231	3.23	0.941
3		0.3	4.46	0.966

Intraparticle diffusion model

Composite	Dye	Rate constant $k_{i\tau}$/ mg g^{-1} min$^{-0.5}$	Initial adsorption rate K_s/ min^{-1}	R^2
1	Congo red	0.27	0.132	0.981
2		0.625	0.1771	0.982
3		0.6	0.098	0.966
1	Methylene blue	0.23	0.1195	0.909
2		0.51	0.0835	0.914
3		0.55	0.1297	0.967

An analysis of the Freundlich adsorption isotherms (Table 3) reveals that the obtained experimental data satisfactorily correspond to this model, since the linear correlation coefficient R^2 > 0.93. The values of the Freundlich constants within the framework of the description of this model characterize the resulting composites as sorbents with satisfactory adsorption properties and the constant $1/n$ characterizes their surface as the inhomogeneous one. Note, that composite **2** has the most heterogeneous surface average sorption properties, while composite **3** has an average surface heterogeneity with good adsorption properties, which is confirmed by the curves of the degree of adsorption *vs*. the exposure time, while mediocre adsorption characteristics using the Freundlich model were obtained for composite **1**. An analysis of the parameters of the Langmuir and Temkin models allows us to conclude that they describe the processes under investigation quite well, since the R^2 values are high, though lower than their counterparts for the Freundlich model. The data in Table 3 demonstrate that the adsorption mechanism differs for the obtained composites. For composite **1** it is physical adsorption, while composite **3** reveals chemisorption with a high heat of the process. Composite **2** is characterized by an intermediate character demonstrating

Table 3 Parameters of the Freundlich, Langmuir and Temkin adsorption models.

Freundlich model

Composite	Dye	$1/n$	K_F	R^2
1	Congo red	0.7	0.33	0.972
2		2.9	0.29	0.996
3		1.28	0.57	0.935
1	Methylene blue	0.62	0.34	0.966
2		2.6	0.25	0.993
3		1.88	0.52	0.959

Langmuir model

Composite	Dye	Maximum adsorption capacity q_{max}/mg g^{-1}	K_L/dm^3 g^{-1}	R_L	R^2
1	Congo red	143.2	0.151	0.24	0.931
2		78.4	0.064	0.43	0.994
3		128.1	0.018	0.73	0.932
1	Methylene blue	81.3	0.271	0.15	0.902
2		111.7	0.036	0.58	0.982
3		166.5	0.0115	0.81	0.995

Temkin model

Composite	Dye	K_T/dm^3 g^{-1}	B/J mol^{-1}	R^2
1	Congo red	0.04	253	0.879
2		0.01	84.7	0.99
3		20.1	697.2	0.973
1	Methylene blue	0.05	185	0.952
2		0.4	412.4	0.944
3		15.7	938.9	0.988

physical sorption with the anionic Congo red dye and a process close to chemical interaction with the cationic methylene blue one.

In summary, the developed single-step method for *in situ* production of composites based on Cu-containing MOF and activated carbons from the tea and coffee waste is simple and industrially applicable. The composites satisfactorily adsorb organic dyes from aqueous solutions and can compete with other similar materials both in terms of adsorption efficiency and ease of preparation. The materials are characterized by porous structure with blocks of activated carbon coated by the MOF microcrystals. Adsorption of Congo red on them has the nature of a physical process, while for methylene blue it respresents physical sorption for composite **1**, chemisorption for composite **3** and their combination for composite **2**. Thus, these materials are promising for extraction of pollutants from the environmental media.

References

1 C.-X. Chen, B. Huang, T. Li and G.-F. Wu, *BioResources*, 2012, **7**, 5109.

2 S. Hirunpraditkoon, N. Tunthong, A. Ruangchai and K. Nuithitikul, *Int. J. Chem. Mol. Eng.*, 2011, **5**, 491.

3 Y. Sun, H. Li, G. Li, B. Gao, Q. Yue and X. Li, *Bioresour. Technol.*, 2016, **217**, 239.

4 M. E. Fernandez, B. Ledesma, S. Román, P. R. Bonelli and A. L. Cukierman, *Bioresour. Technol.*, 2015, **183**, 221.

5 P. Nowicki, J. Kazmierczak-Razna and R. Pietrzak, *Mater. Des.*, 2016, **90**, 579.

6 H. Sayğılı and F. Güzel, *Ecotoxicol. Environ. Saf.*, 2016, **131**, 22.

7 A. C. Martins, O. Pezoti, A. L. Cazetta, K. C. Bedin, D. A. S. Yamazaki, G. F. G. Bandoch, T. Asefa, J. V. Visentainer and V. C. Almeida, *Chem. Eng. J.*, 2015, **260**, 291.

8 M. Song, B. Jin, R. Xiao, L. Yang, Y. Wu, Z. Zhong and Y. Huang, *Biomass Bioenergy*, 2013, **48**, 250.

9 N. Boudechiche, M. Fares, S. Ouyahia, H. Yazid, M. Trari and Z. Sadaoui, *Microchem. J.*, 2019, **146**, 1010.

10 L. Ding, B. Zou, W. Gao, Q. Liu, Z. Wang, Y. Guo, X. Wang and Y. Liu, *Colloids Surf., A*, 2014, **446**, 1.

11 M. Lewoyehu, *J. Anal. Appl. Pyrolysis*, 2021, **159**, 105279.

12 O.-u. Trakoolsa and W. Yoochatchaval, *EnvironmentAsia*, 2020, **13**, 46.

13 S. Na, S. Lee and S. Youn, *Symmetry*, 2021, **13**, 619.

14 E. Hegnsholt, S. Unnikrishnan, M. Pollmann-Larsen, B. Askelsdottir and M. Gerard, *Tackling the 1.6-Billion-ton Food Loss and Waste Crisis*, The Boston Consulting Group, Copenhagen, 2018.

15 L. Zhu, L. Meng, J. Shi, J. Li, X. Zhang and M. Feng, *J. Environ. Manage.*, 2019, **232**, 964.

16 C. M. Oliva González, A. de M. N. Tellez, B. I. Kharisov, O. V. Kharissova, T. E. S. Quezada and L. T. González, *Mendeleev Commun.*, 2021, **31**, 91.

17 O. V. Kharissova, V. A. Zhinzhilo, M. A. Chernomorova, I. E. Uflyand, I. G. de la Fuente and B. I. Kharisov, *Mendeleev Commun.*, 2021, **31**, 893.

18 Z. Liu, A. Fan and C.-H. Ho, *J. Environ. Eng.*, 2020, **146**, 04020018.

19 N. M. Mahmoodi, M. Taghizadeh and A. Taghizadeh, *J. Mol. Liq.*, 2019, **277**, 310.

20 M. Hasanzadeh, A. Simchi and H. S. Far, *J. Ind. Eng. Chem.*, 2020, **81**, 405.

21 G. I. Dzhardimalieva, R. K. Baimuratova, E. I. Knerelman, G. I. Davydova, S. E. Kudaibergenov, O. V. Kharissova, V. A. Zhinzhilo and I. E. Uflyand, *Polymers*, 2020, **12**, 1024.

Received: 30th April 2022; Com. 22/6889